JOURNAL OF GEOPHYSICAL RESEARCH: OCEANS, VOL. 118, 3795–3806, doi:10.1002/jgrc.20281, 2013

Early summer iron limitation of phytoplankton photosynthesis in the Scotia Sea as inferred from fast repetition rate fluorometry

Jisoo Park,[1] Taewook Park,[2] Eun Jin Yang,[1] Dongseon Kim,[2] Maxim Y. Gorbunov,[3] Hyun-Cheol Kim,[1] Sung Ho Kang,[1] Hyoung Chul Shin,[1] SangHoon Lee,[1] and Sinjae Yoo[2]

Received 1 February 2013; revised 21 May 2013; accepted 18 June 2013; published 2 August 2013.

[1] We describe variability in the phytoplankton physiological status in the west Scotia Sea of the Southern Ocean in the early austral summer prior to and at the beginning of a phytoplankton bloom. This area is characterized by high concentrations of major nutrients (such as nitrate, phosphate, and silicate), but exhibit chronically low concentrations of dissolved iron and deep vertical mixing. Using a fast repetition rate fluorometry, we measured photosynthetic characteristics of phytoplankton in the euphotic zone. These measurements provide an express diagnostic of the effects of environmental factors, including iron limitation, on photosynthetic processes. The quantum yields of photochemistry in Photosystem II (F_v/F_m) in subsurface phytoplankton were, on average, 40% lower than the maximum values for nutrient-replete communities. Higher values of F_v/F_m were observed in the frontal mixing zone that may have been caused by the induction of iron into the euphotic layer. Our results suggest physiological signatures of iron limitation of photosynthesis in the western Scotia Sea in the early austral summer. The data imply that, together with light conditions and grazing pressure, iron availability may be important for phytoplankton growth in the Scotia Sea even in the early summer.

Citation: Park, J., T. Park, E. J. Yang, D. Kim, M. Y. Gorbunov, H.-C. Kim, S. H. Kang, H. Chul Shin, S. Lee, and S. Yoo (2013), Early summer iron limitation of phytoplankton photosynthesis in the Scotia Sea as inferred from fast repetition rate fluorometry, *J. Geophys. Res. Oceans*, *118*, 3795–3806, doi:10.1002/jgrc.20281.

1. Introduction

[2] Despite permanently high concentrations of inorganic macronutrients [*Garcia et al*., 2006; *Mitchell and Holm-Hansen*, 1991] and seasonally high light inputs, the majority of surface waters in the Southern Ocean (SO) are characterized by low chlorophyll levels (typically <1.5 mg m^{-3}) [*Arrigo et al*., 1998; *Marrari et al*., 2006] and low rates of primary production [*Barbini et al*., 2003; *El-Sayed*, 2005]. Oceanographic research over the last decade revealed that low chlorophyll-a concentrations and low productivity in nutrient-rich surface waters of the SO result from a deficiency of iron [*de Baar et al*., 1995, 2005; *Hopkinson et al*., 2007; *Martin and Fitzwater*, 1988; *Wulff and Wängberg*, 2004]. Iron fertilization experiments in the SO have clearly demonstrated that iron enrichment increased algal photosynthetic competence, quantum yields of photosynthesis, growth rates, chlorophyll biomass, nitrate uptake, and altered algal community structure toward dominance of diatoms [*Boyd*, 2002; *Coale et al*., 2004; *Gervais et al*., 2002; *Hiscock et al*., 2008; *Hopkinson et al*., 2007; *Olson et al*., 2000; *Petrou et al*., 2011]. Most iron enrichment experiments in the SO have been conducted in mid or late austral summer, but the physiological status of phytoplankton at the beginning in early summer has scarcely been reported.

[3] Mesoscale patches of high chlorophyll concentration/productivity often occur in frontal regions [*Froneman et al*., 2001; *Holm-Hansen et al*., 2004; *Laubscher et al*., 1993], coastal/neritic waters [*Arrigo and McClain*, 1994; *Holm-Hansen and Mitchell*, 1991], the Marginal Ice Zone [*Froneman et al*., 2001; *Sullivan et al*., 1993; *Westwood et al*., 2010], and polynyas [*Arrigo and van Dijken*, 2003; *Moore and Abbott*, 2000; *Smith and Gordon*, 1997]. These "naturally fertilized" waters have been considered as most productive and biologically important areas of the SO [*Blain et al*., 2007; *Mongin et al*., 2008]. *Blain et al*. [2007] suggested that the efficiency of natural iron fertilization from below the euphotic zone to the surface may be 10 times higher than the previous estimates obtained from short-term artificial iron-addition experiments. Recently, *Park et al*. [2010] argued that the dynamics of natural iron fertilization in the southwest Atlantic sector of the SO is driven by topographic effects that are responsible for a weak seasonality of the phytoplankton bloom and a strong interannual variability in that region.

Additional supporting information may be found in the online version of this article.

[1]Korea Polar Research Institute, Incheon, South Korea.
[2]Korea Institute of Ocean Science and Technology, Ansan, Seoul, South Korea.
[3]Institute of Marine and Coastal Sciences, Rutgers, the State University of New Jersey, New Brunswick, New Jersey, USA.

Corresponding author: M. Y. Gorbunov, Institute of Marine and Coastal Sciences, Rutgers, the State University of New Jersey, 71 Dudley Rd., New Brunswick, NJ 08901, USA. (gorbunov@marine.rutgers.edu)

2169-9275/13/10.1002/jgrc.20281

[4] Iron plays a key role in the photosynthetic electron transport in algal cells [*Raven et al*., 1999]. Development and improvement of physiological or chemical diagnostics of nutrient stress and, in particular, of iron limitation have been a continuing goal of the oceanographic community [*Hopkinson et al*., 2007]. Active fluorescence techniques have been used to probe the function of photosynthetic light harvesting, photosystem II (PSII) photochemistry, and electron transport [*Kolber et al*., 1988]. The fluorescence yield from PSII is highly variable and dependent on the physiological state of phytoplankton, and is affected by environmental factors, including light and nutrient availability [*Falkowski and Kolber*, 1995]. Fast repetition rate (FRR) fluorometry is a nondestructive and rapid method, and it has been used to monitor variations in the quantum efficiency of PSII (F_v/F_m) and the functional absorption cross-section of PSII (σ_{PSII}) [*Falkowski and Kolber*, 1995; *Kolber and Falkowski*, 1993]. Variable fluorescence signals are particularly sensitive to iron limitation [*Greene et al*., 1992; *Vassiliev et al*., 1995] and can be used to monitor alterations in the physiological state of phytoplankton in response to iron stress [*Falkowski et al*., 2004].

[5] Variable fluorescence measurements can be used to assess iron limitation without conducting incubations [*Olson et al*., 2000]. However, the paucity of studies of phytoplankton physiology in relation to iron supply is attributed to the difficult accessibility of the SO. A recent study showed that phytoplankton iron stress is an important control on photosynthetic physiology in the southern Drake Passage [*Hopkinson et al*., 2007]. Their incubation experiments suggested that mixing between iron-limited Antarctic circumpolar current (ACC) waters and iron-replete shelf waters in the southern Drake Passage may stimulate high phytoplankton biomass in the areas downstream of the mixing region. *Dulaiova et al*. [2009] also emphasized the importance of lateral mixing, which provides ample iron supply to account for the biological demand of dissolved iron to the offshore regions of the Drake Passage. The authors found that lateral fluxes of iron overwhelm vertical inputs and vertical export from the water column, but quantitative contributions of these fluxes to the regulation of iron supply in the upper water column requires further investigation.

[6] Here, we report results of a multidisciplinary study in the Drake Passage and the western part of the Scotia Sea in the early austral summer of 2001 (30 November to 9 December), conducted as a part of the Korea Antarctic Research Program (KARF 15th). The Drake Passage is located south of South America, and the ACC flow is the strongest in this area. The Polar Front is located circa 57 to 63°S in the Drake Passage [*Moore et al*., 1999], and this area is known to be a typical high nutrient low chlorophyll (HNLC) region. However, in the shelf zone and near the Antarctic Peninsula, high chlorophyll concentrations seasonally appear due to the effects of water inflow from the Bellingshausen Sea and the Weddell Sea. Weak seasonality and strong interannual variations of phytoplankton blooms prevailed in the Scotia Sea, except for the western part of the Drake Passage region [*Park et al*., 2010]. The main entrainment of upwelled Upper Circumpolar Deep Water, which can cause a large iron flux into the surface layer, occurs in autumn and winter [*Hoppema et al*., 2003]. *Smith et al*. [2000] suggested that phytoplankton biomass and primary productivity in the Ross Sea was likely limited by low irradiance in the early spring, but was limited by trace-metal availability in the late spring and summer. If low irradiance, but not iron deficiency, would be a primary limiting factor in the Scotia Sea in early summer, one would expect no physiological signatures of iron limitation at that time.

[7] The objective of our field study was to elucidate the natural variability in phytoplankton photosynthetic characteristics as an index of iron limitation in the western part of the Scotia Sea in early summer and to relate this variability to physicochemical conditions of the water column. We report here the physiological state of phytoplankton and environmental conditions in the western Scotia Sea before and at the beginning of a phytoplankton bloom.

2. Methods

2.1. Observations

[8] The cruise was conducted in a region located between 52–63°S and 66–52°W and included the Drake Passage, the western Scotia Sea, the northeastern Antarctic Peninsula, and the Bransfield Strait (Figure 1 and Table 1) in the early austral summer of 2001 aboard R/V Yuzhmorgeologiya. Stations (23 total) were located across three major fronts: the Polar Front (PF), the Southern Antarctic circumpolar current front (SACCF), and the Southern Boundary (SB) of the ACC. Figure 1 shows the monthly composite surface chlorophyll-a image from sea-viewing wide field-of-view sensor (SeaWiFS) level-3 data (version

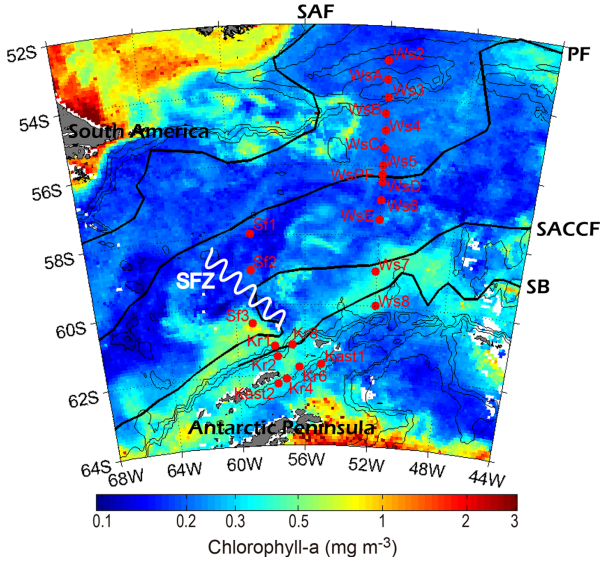

Figure 1. Monthly composite chlorophyll-a image (SeaWiFS level 3 data) for the month of December 2001, together with station locations for the Korea Antarctic Research Program 15th cruise. Black thin lines indicate 1000, 2000, and 3000 m isobaths. Four thick lines show approximate locations of the sub-Antarctic Front, Polar Front (PF), Southern Antarctic Circumpolar Current Front (SACCF), and southern boundary of the ACC (after *Orsi et al*. [1995] and *Moore et al*. [1997]; see also *Meredith et al*. [2003]).Shackleton Fracture Zone (white zigzag line) is also depicted as a major topographic barrier for the ACC.

Table 1. Locations of 23 Stations With Dates and Local Time (= UTC-3h) for Observation

Station	Latitude (°S)	Longitude (°W)	Local Date	Local Time
Ws2	52.98	52.05	30 Nov	20:30
WsA	53.51	52.00	1 Dec	06:31
Ws3	54.03	51.94	1 Dec	10:50
WsB	54.49	52.01	1 Dec	16:39
Ws4	54.97	51.98	2 Dec	22:07
WsC	55.49	51.99	2 Dec	05:28
Ws5	55.97	52.01	2 Dec	10:38
WsD	56.45	51.98	2 Dec	17:19
WsPF	56.22	52.00	2 Dec	20:26
Ws6	56.97	52.00	3 Dec	04:32
WsE	57.52	52.01	3 Dec	13:08
Ws7	59.01	52.08	4 Dec	01:26
Ws8	59.99	51.99	4 Dec	14:00
Sf1	57.95	58.99	5 Dec	14:40
Sf2	58.98	59.04	6 Dec	02:25
Sf3	60.50	59.02	6 Dec	15:11
Kr1	61.17	57.79	6 Dec	23:01
Kr2	61.47	57.62	7 Dec	2:40
Kr4	62.11	57.13	7 Dec	10:04
Kr6	61.78	56.33	7 Dec	21:30
Kr8	61.13	56.76	8 Dec	03:03
Kast1	61.69	55.02	8 Dec	11:44
Kast2	62.25	57.61	8 Dec	15:10

2010.0), together with bottom topography (1000, 2000, and 3000 m isobaths) and major fronts. The Shackleton Fracture Zone is also depicted as a major topographic barrier for the ACC in the region.

[9] Temperature, salinity, and underwater light intensity were measured using a Sea-Bird conductivity, temperature, and depth probe (CTD) equipped with a submersible photosynthetically available radiation (PAR) sensor (Biospherical Instruments Inc. QSP-200L). Water samples were taken from standard depths (surface, 10, 20, 30, 50, 75, 100, and 150 m, respectively) using 10 L Niskin bottles mounted on the CTD-rosette. Chlorophyll-a concentrations were measured following the fluorometric method [*Parsons et al*., 1984] with a Turner fluorometer (TD-700 model) on board the ship. The instrument was calibrated against a commercial chlorophyll-a standard (Turner Designs Inc.). We filtered 500 mL of water through Whatmann GF/F filter that was then soaked in 90% acetone for 24 h prior to absorption measurements. Two size fractions of phytoplankton, nanoplankton (<20 μm), and microplankton (>20 μm) were gently separated by serial filtration (without vacuum pressure). Then, nanofraction chlorophyll-a concentrations were measured in the same way as bulk populations.

[10] Water samples for nutrient analysis were poured directly from Niskin bottles into acid cleaned polyethylene bottles, and the samples were maintained in a freezer (<−20°C) until analysis. Nutrient concentrations were measured using an automatic ion analyzer (LaChat model, QuikChem AE) and samples were validated against a standard seawater sample (Wako Pure Chemical Industries, CSK (Cooperative Study of the Kuroshio and Adjacent Regions) standard solution).

[11] For analysis of the phytoplankton community structure, a CTD-Niskin rosette sampler was also used to take water samples from 10 m depth. Aliquots of 125 mL were preserved with glutaraldehyde (1% final concentration). Sample volumes of 100 mL were filtered through Gelman filter paper (0.45 μm pore size, 25 mm diameter). The filters were mounted on microscope slides with water-soluble embedding medium (HPMA, N-(2-hydroxypropyl)methacrylamide) on board [*Crumpton*, 1987; *Kang et al*., 2001]. Then, HPMA slides were examined using light microscopy (LM) and epifluorescence microscopy (Nikon type 104). Cells were counted in random fields until 300–500 had been observed in total. Most *Phaeocystis* cells present were of the solitary form. Solitary *Phaeocystis* cells were distinguished from other autotrophic flagellates based on cell size (3–5 μm) and shape, and the presence of flagella. To estimate phytoplankton carbon biomass, biovolume was calculated based on the size of each cell using an image analyzer with a camera mounted on the microscope. Biovolume was then converted to biomass according to *Menden-Deuer and Lessard* [2000].

2.2. Determination of Photochemical Parameters

[12] A Chelsea Instruments FASTtracka FRR fluorometer was used to measure variable fluorescence of phytoplankton from discrete samples. After collection from Niskin bottles, samples were kept at in situ temperature in amber glass bottles for 30 min for low-light adaptation and recovery from nonphotochemical quenching. Test measurements of dark fluorescence recovery showed that longer adaptation did not affect, within ∼5% precision, the fluorescence readings, suggesting that a 30 min interval was sufficient for full recovery. Analysis of vertical profiles of FRRF fluorescence showed that F_v/F_m values recorded in surface samples were as high as those deeper in the mixed layer, also suggesting full recovery from photoinhibition and nonphotochemical quenching.

[13] The FRR fluorometer was programmed to generate a saturating Single Turnover Flash consisting of 100 subsaturating flashlets (each 1.1 μs long followed at a 50% duty cycle). PSII parameters such as the minimal fluorescence yield (F_0; when all reaction centers are open), the maximal fluorescence yield (F_m; all reaction centers are closed), the functional (or effective) absorption cross-section of PSII (σ_{PSII}) were measured as described in *Kolber et al*. [1988]. The Chelsea FRS program (version 1.8) was used for post-processing of acquired data. The F_v/F_m was calculated as a ratio of variable fluorescence ($F_v = F_m - F_0$) to the maximum one (F_m). Fluorescence measurements were corrected for the blank signal recorded from filtered seawater as described in *Bibby et al*. [2008]. We made 10 replicates and then calculated the average value and standard deviation.

2.3. Physical Environments

[14] Under conditions of light winds and solar warming, SST variations of 1 or 2°C can occur within the first 1–2 m near the surface [*Price et al*., 1986]. Therefore, we chose 10 m as our reference depth to avoid diurnal cycles in the top few meters of the water column. The mixed layer depth (MLD) was defined as the depth at which the potential density is equivalent to that at 10 m and a 0.2°C decrease in temperature from 10 m depth. This definition has been widely employed in previous studies [*Breugem et al*., 2008].

[15] To investigate similarity of a given water mass to the ACC or shelf waters, we examined a water index (WI) following *Zhou et al*. [2010]:

$$WI = \frac{1}{2Z}\int_0^Z \left\{ \left(\frac{T - T_A}{T_s - T_A}\right)^2 + \left(\frac{S - S_A}{S_s - S_A}\right)^2 \right\}^{\frac{1}{2}} dz$$

where T is the temperature, S is the salinity, and Z is the depth of the water column. The subscript A and S represent reference stations—Ws2 (ACC water) and Kast1 (Shelf water), respectively.

3. Results

3.1. Hydrography and Chlorophyll Distributions

[16] The SeaWiFS chlorophyll-a image of the study region for December of 2001, together with station locations, is shown in Figure 1. During the cruise, surface chlorophyll-a concentrations (determined on water samples) were relatively low in the ACC region (0.16–0.36 mg m^{-3}), but high in other regions (0.52–2.06 mg m^{-3}). A major transition in surface chlorophyll concentrations occurred near the SACCF, with the shift toward high chlorophyll waters in the south. High chlorophyll concentrations near the Sf3 station in the satellite image seems to be the bloom developed after the cruise (i.e., in mid or late December). A time series of SeaWiFS chlorophyll maps of the study area (not shown) revealed that the sampling period was just preceding the spring bloom in the western Scotia Sea. The bloom peaked in mid-January of 2002, i.e. a month after the cruise.

[17] Figure 2 shows profiles of temperature, salinity and chlorophyll-a concentration measured from the water samples in the upper water column at 23 stations. Generally, the MLDs were >50 m, with the exception of Ws5, WsD, Ws6, Sf1, Kr1, and Kr2 stations located near the fronts. MLD ranged from 16 (WsD) to 110 m (Kr6). The uniform water column structure in the center of the PF during the cruise was unexpected. However, subsurface chlorophyll maximums (SCMs) were clearly seen in WsPF, Ws6, Sf1, Sf3, and Kr1 stations. In addition, a distinct chlorophyll maximum at the surface was observed at Ws7, Ws8, Kr4, Kr6, and Kast2 stations. Generally, the width of the Antarctic PF is about 43 km [*Moore et al*., 1999] and the PF is defined by sea surface temperature of around 1.5°C or by the northern limit of the temperature minimum layer. In this study, the surface temperature at the PF station was somewhat higher (2.77°C; probably it was not exactly in center of the PF), but the temperature minimum layer (ca., 80–140 m) was repeatedly observed at the stations south off the PF (Ws6, WsE, Ws7, Sf1, Sf2, Sf3, and Kr1 stations) [see also *Holm-Hansen et al*. 2004].

[18] For the purpose of comparison, the study area was divided into three regions, based on the hydrographic characteristics [*Moore et al*., 1997; *Orsi et al*., 1995]. The regions were defined as follows: (1) ACC waters north off PF and PF station, (2) ACC waters south off PF, and (3) shelf and the Southern Boundary of the ACC.

3.2. ACC Waters North Off Polar Front Region and PF Station

[19] Eight stations belong to this region (Ws2, WsA, Ws3, WsB, Ws4, WsC, Ws5, and WsPF). Surface water temperatures were moderately high and ranged from 5.25°C to 2.77°C (north to south). Surface chlorophyll-a concentrations were very low (0.17–0.28 mg m^{-3}). Vertical distributions of F_v/F_m, σ_{PSII}, and chlorophyll-a concentration (averaged over the three stations, Ws2, Ws5, and WsPF, with standard deviations) are shown in Figure 3 (left). SCMs were found at ca. 50 m depth at Ws5 and WsPF stations, though MLD was as deep as 93 m at the WsPF. The surface values of F_v/F_m varied from 0.3 at Ws5 and WsPF to 0.42 at Ws2 (Table 2). Values of F_v/F_m increased with depth and reached the maximum of about 0.57 below 100 m. σ_{PSII} also increased with depth by SCM, but decreased below SCM.

3.3. ACC Waters South Off Polar Front Region

[20] Three stations in the western Scotia Sea (WsD, Ws6, and WsE) and another three stations in the Drake Passage across the Shackleton Transverse Ridge (Sf1, Sf2, and Sf3) belong to this region. Surface temperatures ranged from 0.47 to 1.64°C and surface chlorophyll-a concentrations were also low (0.17–0.36 mg m^{-3}). Among these stations, we measured FRRF parameters only at three stations, Sf1, Sf2, and Sf3 (Table 2). SCMs were also found at ca. 50 m depth at Sf1 and Sf3 stations and at ca. 100 m at Sf2 station. F_v/F_m value at the surface was high at Sf2 (0.52), but was low at Sf1 (0.25) and Sf3 (0.35). F_v/F_m increased with depth, except Sf2 where F_v/F_m was high throughout the entire water column.

3.4. Shelf and the Southern Boundary of the ACC Region

[21] Seven stations in the shelf around South Shetland Islands (Kr1, Kr2, Kr4, Kr6, Kr8, Kast1, and Kast2) and two stations in the southwestern Scotia Sea (Ws7 and Ws8) were attributed to this region. Surface temperatures ranged from 0.20 (Kr8) to 0.79°C (Ws7) and sea surface chlorophyll-a concentrations were relatively high (~0.50–2.0 mg m^{-3}). FRRF parameters have been measured at three stations in the shelf region (Kr4, Kr6, and Kast1) and at two stations in the Southern Boundary of the ACC (Ws7 and Ws8) (Figure 3). MLDs were deep (>68 m) and no SCMs were observed. Surface F_v/F_m values ranged from 0.32 to 0.51, and were intermediate between the low values found in ACC waters and the highest values found at Sf2 station (Table 2). At all stations, F_v/F_m increased with depth. σ_{PSII} was vertically homogeneous at all stations except Ws7, and this was probably attributed to a weak stratification of the water column in this region.

3.5. Nutrients and Phytoplankton Communities

[22] Vertical distributions of nitrate + nitrite, phosphate, and silicate concentrations in the three regions are shown in Figure 4. All macronutrient concentrations were high even at the surface at all stations (Table 2 and Figure 4). The minimum amount of nitrate + nitrite was observed at Ws2 station (22.9 μM kg^{-1}), and the maximum was 28.5 μM kg^{-1} at Kast1. The phosphate and silicate concentrations also were lowest at Ws2, and highest at the southern stations (especially silicate concentrations). Vertically, gradients of nutrient concentration increases with depth were much larger in the ACC waters south of Polar Front region than in the ACC waters north of Polar Front region or the shelf and the Southern Boundary of the ACC. A notable feature of the chemical properties was that the major nutrients were saliently high on the surface at Sf2 and were

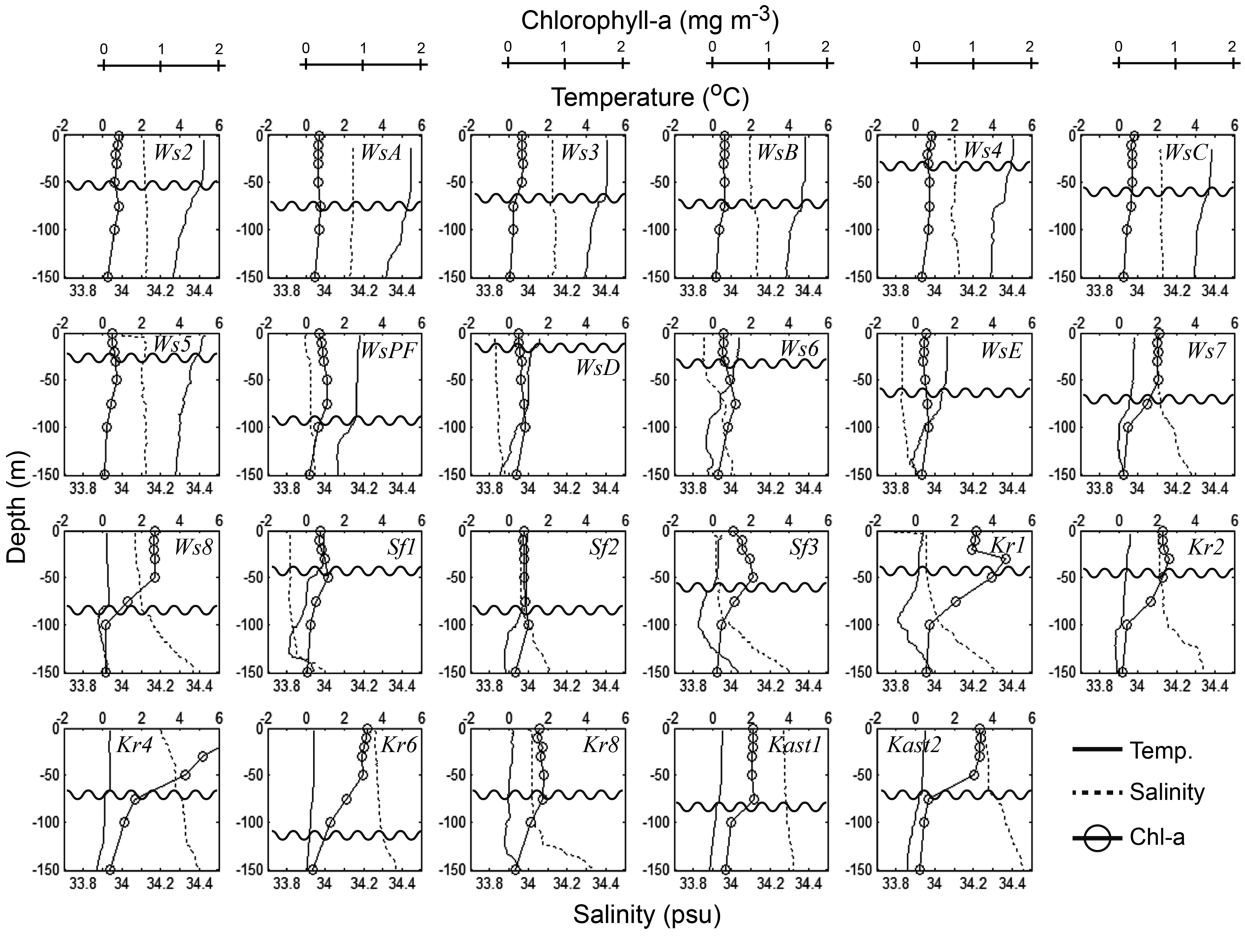

Figure 2. Vertical profiles of temperature, salinity, and chlorophyll-a concentration at 23 stations. Horizontal wavy lines show the mixed layer depths.

more uniform with depth. In addition, nitrate + nitrite and phosphate concentrations in the Southern Boundary of the ACC (Ws7 and Ws8) were as high as in the shelf, but silicate concentrations were not.

[23] The PF marks the location with strong meridional gradients in both temperature and nutrients (Figure 5). In contrast, low levels of surface chlorophyll-a concentration prevailed not only in the ACC waters north off PF, but also

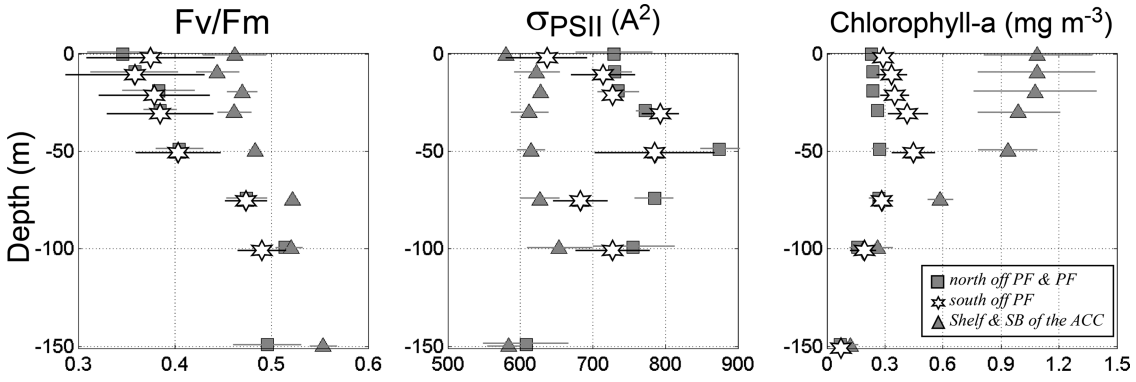

Figure 3. Vertical profiles of F_v/F_m, the functional absorption cross section of PSII (σ_{PSII}), and chlorophyll-a concentration in three distinct regions of the Scotia Sea: ACC waters north off PF and PF station, ACC waters south off PF, and Shelf and the Southern Boundary of the ACC. Profiles for the first region represent the averaged values over stations Ws2, Ws5, and WsPF; the second region—Sf1, Sf2, and Sf3; the third region—Kr4, Kr6, Kast1, Ws7, and Ws8. Horizontal lines show the range of variability (standard deviations) in respective parameters in each region.

Table 2. Physiological Parameters of Near-Surface Phytoplankton and Nutrient Concentrations in Various Regions of the Scotia Sea[a]

Sts.	Region	Temp	MLD	F_o	F_m	F_v/F_m	σ_{PSII}[b]	TN[c]	P[c]	Si[c]	Chl-a	<20
Ws2	North to pf	5.25	55	1.100	1.920	0.426	680	22.9	1.65	14.4	0.284	87
Ws5	North to pf	5.31	24	0.667	0.995	0.330	656	23.6	1.75	17.4	0.168	93
WsPF	PF	2.77	93	1.650	2.300	0.283	852	25.6	1.85	20.9	0.240	58
Sf1	South to pf	0.94	41	1.790	2.400	0.253	760	24.1	1.72	30.2	0.248	50
Sf2	South to pf	0.93	82	0.723	1.500	0.517	609	28.1	2.11	63.6	0.260	37
Sf3	South to pf	0.47	55	0.927	1.430	0.351	540	25.7	1.87	50.0	0.360	74
Kr4	Shelf	0.42	70	5.280	7.830	0.325	711	27.3	2.13	102.7	2.060	54
Kr6	Shelf	0.40	110	2.750	4.690	0.415	570	27.9	2.13	99.8	1.068	40
Kast1	Shelf	0.52	79	1.350	2.340	0.424	508	28.5	2.19	100.2	0.708	86
Ws7	SB	0.79	68	1.500	3.050	0.508	589	28.4	2.17	79.6	0.696	66
Ws8	SB	0.24	82	2.440	3.820	0.361	803	28.3	2.20	84.6	0.904	88

[a]Temperature (°C), mixed layer depth (MLD, m), FRRF parameters (F_0, F_m, F_v/F_m, and σ_{PSII}), nitrate + nitrite (TN), phosphate, silicate, chlorophyll-a concentration (mg m^{-3}), and percentage of <20 μm size-fractionated chlorophyll-a (%).
[b]Units are A^2.
[c]All units are μM kg^{-1}.

in the ACC waters south off PF and PF station region. The surface chlorophyll-a concentrations were highest in Kr4 (~2.0 mg m^{-3}), and moderately high in another shelf and the Southern Boundary of the ACC region (0.5–1.0 mg m^{-3}). The nanofraction (<20 μm) of chlorophyll-a accounted for 37 to 96% of total chlorophyll-a concentration, with the smallest values observed in the shelf region. The percentage of nanofraction was >80% in most ACC waters except WsPF, Sf1, and Sf3 stations (Figure 5). The nanofraction of chlorophyll-a was also high at Ws7 and Ws8 stations (86.2% and 95.6%, respectively).

[24] The abundance of three dominant phytoplankton assemblages varied considerably among stations (Figure 6). While the nano size flagellate *Phaeocystis* sp. was prevalent in the study area, with its maximum abundance of 2650 cells mL^{-1} observed at the shelf station (Kr4). *Phaeocystis* sp. also prevailed at Sf2 and Ws7 stations (where F_v/F_mvalues were highest at the surface; Table 2) and at Ws8. Diatom (with chain forming diatoms of the genera *Chaetoceros* spp. and *Fragilariopsis* sp.) was abundant in the PF as well as at Sf1 and Sf3. In the shelf and the Southern Boundary of the ACC region, *Cryptomonas* sp. was abundant, with the maximum of 2740 cells mL^{-1} observed at Kr4 (the station of highest surface chlorophyll-a concentration). Outside this region, *Cryptomonas* sp. formed a minor component.

4. Discussion

4.1. Hydrographic Properties

[25] The ACC consists of a number of high-velocity fronts separated by relatively quiescent zones. The meridional position of these Antarctic fronts and the flow of the ACC through the Drake Passage are constrained by local topography [*Sprintall*, 2003]. Our cruise track crossed over three major fronts, including PF, SACCF, and SB. The dynamics of these fronts exerts a strong influence on phytoplankton distribution and productivity [*Laubscher et al.*, 1993]. Generally, the ACC waters are nutrient impoverished, with localized enrichments driven by upwelling or cross-frontal mixing [*Moore and Abbott*, 2000]. These nutrient enrichments could promote phytoplankton growth [*Moore and Abbott*, 2000]. Mixing between the iron-poor Antarctic surface water of the ACC and iron-rich waters from the shelf provides a physical control that could be responsible for enhanced primary productivity in the

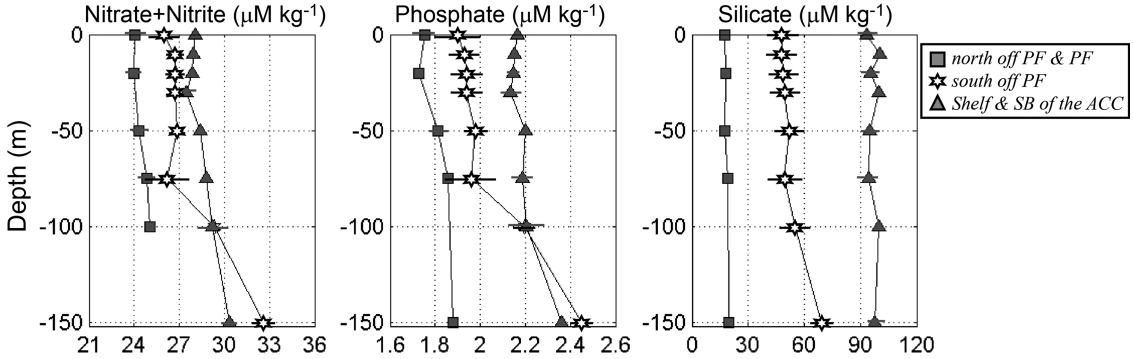

Figure 4. Vertical distributions of concentrations of major nutrients, including (left) nitrate + nitrite, (middle) phosphate, and (right) silicate in three distinct regions of the Scotia Sea: ACC waters north off PF and PF station, ACC waters south off PF, and Shelf and the Southern Boundary of the ACC. Profiles for the first region represent the averaged values over stations Ws2, Ws5, and WsPF; the second region—Sf1, Sf2, and Sf3; the third region—Kr4, Kr6, Kast1, Ws7, and Ws8. Horizontal lines show the range of variability (standard deviations) in respective parameters in each region.

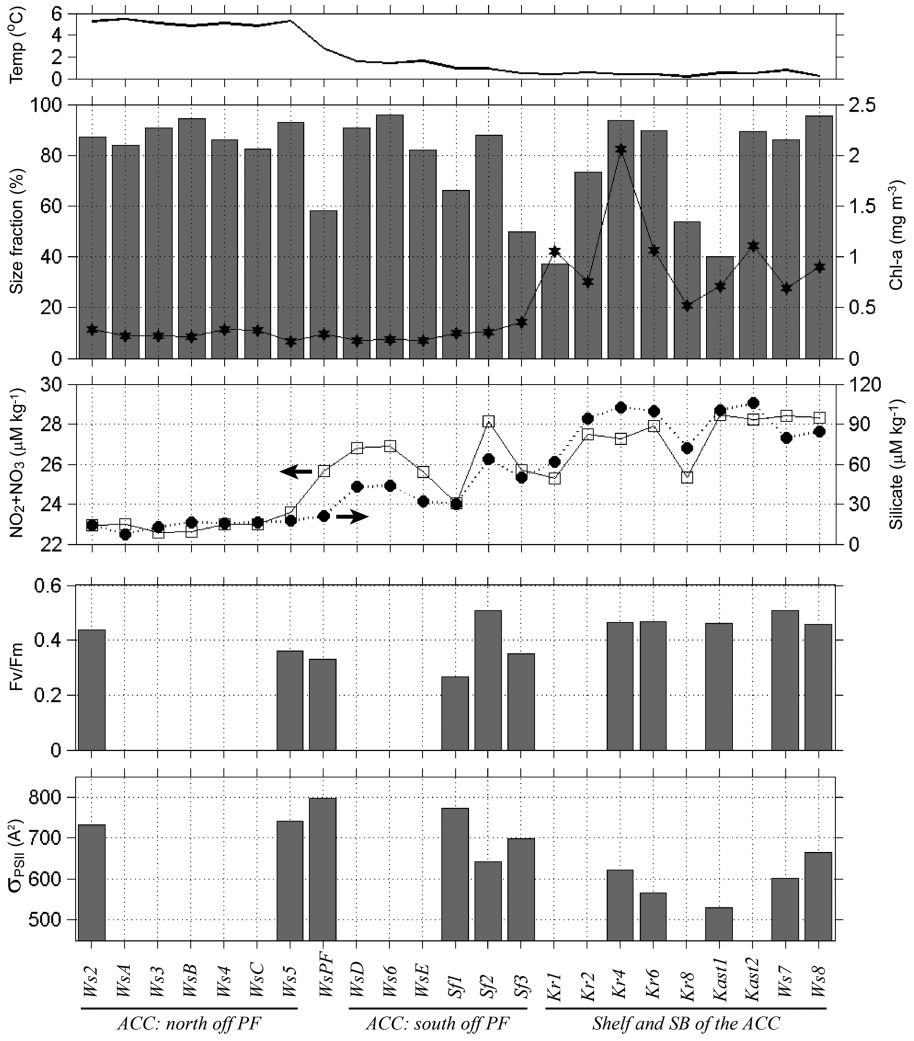

Figure 5. Horizontal variability of physical, chemical, and physiological characteristics across the Scotia Sea, including sea surface temperature; the percentage of smaller size fraction (<20 μm) of phytoplankton (bars) and total chlorophyll-a concentration (line with stars); concentration of major nutrients (nitrate + nitrite and silicate) at the surface; F_v/F_m and the functional absorption cross section of PSII of phytoplankton in the mixed layer.

southwestern Scotia Sea [*Zhou et al*., 2010]. Moreover, Shackleton Jet, which is the southward detour of ACC branch into the Shackleton Gap between the Shackleton Transverse Ridge and Elephant Island, is accelerated further to 70 cm s^{-1} [*Zhou et al*., 2010].

[26] In this study, we classified three regions based on their location relative to the major fronts. To quantify water column properties per se, we further used a WI [*Zhou et al*., 2010] to disclose the hydrological similarity of a given water to the waters of the ACC or of the shelf (Figure 7). We have chosen Ws2 and Kast1 as standards for the ACC and the shelf waters, respectively. When the value of WI is close to 0, the water T-S characteristics are close to that of the ACC; and when WI is close to 1, the water T-S characteristics are close to that of the shelf, and any water with the value of WI between 0 and 1 could be formed as a percentage mixture between the two water masses [*Zhou et al*., 2010].

[27] All values of WI were close to zero in the ACC waters north off PF and PF station region, while most values of WI were around 1 on the shelf, except Kr2 (Figure 7). In addition, all values of WI were >1 in the ACC waters south off PF and PF station region, except Sf2, though Sf2 station was located far from the shelf. Striking differences also were observed at Ws7 and Ws8, which were quite different from not only northern offshore station (WsE) but also stations on the shelf. Although this approach per se is not sophisticated for such a broad area, it is worthwhile to be used to distinguish water column properties from a hydrographical point of view.

4.2. Variability of Photochemical Parameters

[28] Variability in F_v/F_m is generally associated with changes in the physiological state of phytoplankton [*Olaizola et al*., 1996], and inversely correlates with the availability of nutrients, especially iron in the SO [*Boyd and Abraham*, 2001; *Olson et al*., 2000] and in the subarctic Pacific Ocean [*Suzuki et al*., 2002]. During our cruise, the macronutrients were abundant and, thus, were not a

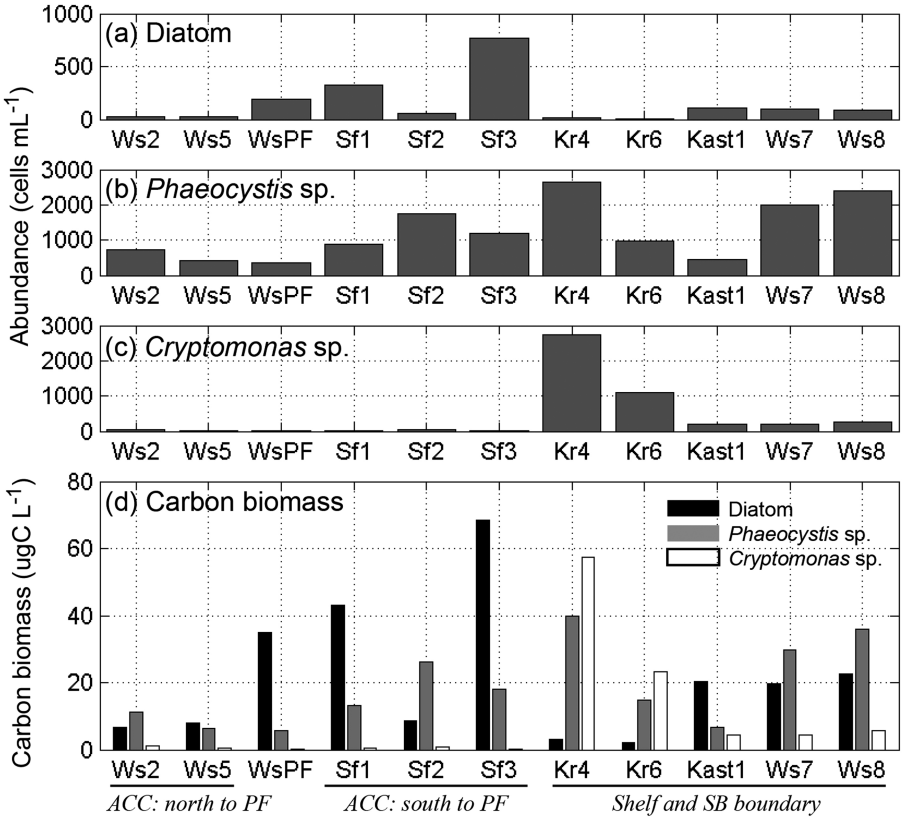

Figure 6. Abundance of three phytoplankton functional groups, including (a) diatoms, (b) *Phaeocystis* sp., and (c) *Cryptomonas* sp., and (d) carbon biomass in the near-surface layer.

limiting factor (Table 2 and Figure 4). Following *Martin et al*. [1990], many studies have shown that low productivity in the nutrient-rich waters of the eastern equatorial Pacific and the SO results from a deficiency of iron. FRRF-derived PSII characteristics, especially F_v/F_m and σ_{PSII}, were found to be sensitive indicators of iron limitation [*Greene et al*., 1992; *Hopkinson et al*., 2007; *Sosik and Olson*, 2002; *Vassiliev et al*., 1995]. The quantum yields of carbon fixation by phytoplankton in the SO are also Fe driven, with low quantum yields being indicative of iron stress [*Hiscock et al*., 2008]. In addition, *Olson et al*. [2000] found significant correlations not only between ambient iron concentrations and F_v/F_m, but also between ambient iron and the response of F_v/F_m to iron enrichment in the SO. Therefore, based on previous lab and field research, we may conclude that the low values of F_v/F_m observed in the upper-layer phytoplankton in our study were indicative of iron stress.

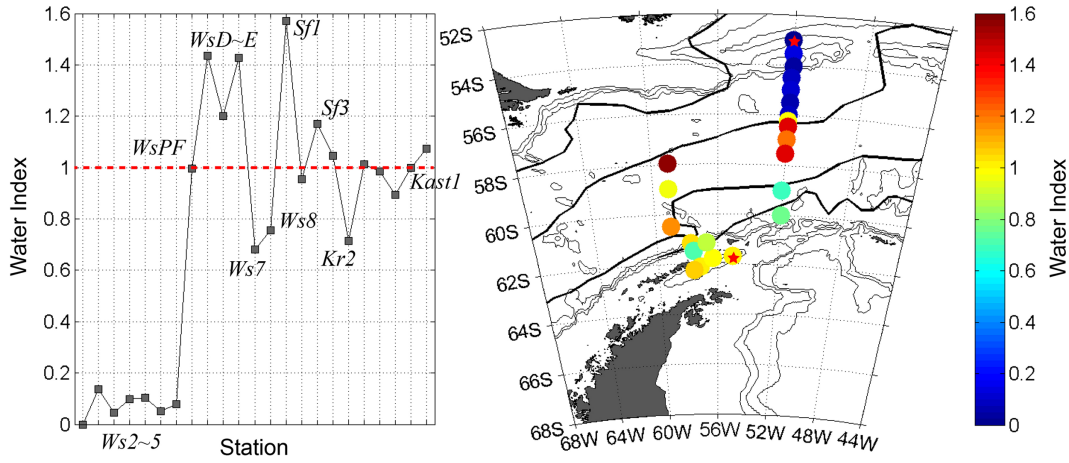

Figure 7. Horizontal distribution of water index across the Scotia Sea. The reference stations for WI calculations, Ws2 (the ACC water), and Kast1 (the Shelf water), are marked with red stars in the right side.

[29] The other factors that may potentially reduce the measured values of photosynthetic efficiency (F_v/F_m) are photoinhibition [*Falkowski et al*., 2004] and grazing by zooplankton [*Fuchs et al*., 2002]. Photoinhibition is attributed to the photodamage of PSII reaction centers by supra-optimal irradiance and observed during the day in the near-surface layer. This effect is dynamic [e.g, *Falkowski et al*., 2004] and usually recovers, within 30–60 min, under low irradiance. Because our measurements were conducted on low-light acclimated samples (see section 2), the effect of photoinhibition was removed. Grazing by zooplankton may reduce the bulk F_v/F_m values due to a fraction of damaged cells (with low F_v/F_m) in the population and due to the presence of pigment degradation products in water. Because the gross photosynthesis and growth rates of phytoplankton are greatly reduced by low light availability at the bottom of the euphotic zone, the effect of grazing, e.g., the amount of pigment degradation products [*Gervais et al*., 2002] should be most pronounced below the mixed layer. Our measured vertical profiles of F_v/F_m showed that F_v/F_m remained high below the mixed layer and decreased in the upper part of the water column. This decrease in F_v/F_m cannot be explained by the effects of grazing. Our data corroborate the results of *Holm-Hansen et al*. [2004] who noted that light availability and grazing have relatively small impact on the spatial variability of phytoplankton biomass of the Scotia Sea, compared to the effects of iron availability.

[30] In the SO, iron may originate from land (continent and islands), melting sea ice [*El-Sayed*, 2005; *Martin et al*., 1990; *Sedwick et al*., 2000; *Sullivan et al*., 1993], and the bottom or deep iron-rich water masses [*Blain et al*., 2007]. In shallow coastal waters around the Antarctic Peninsula, high iron concentrations may be due to runoff from the land or release of iron by resuspension of bottom sediments [*Ardelan et al*., 2010]. Among other sources, melting icebergs can provide substantial inputs of iron [*Smith et al*., 2007], but icebergs were spatially restricted during our study. In contrast, the ACC waters in the central Scotia Sea are considered to be iron-impoverished. The high phytoplankton biomass in the central Scotia Sea might only be speculated as the result of natural iron fertilization by waters from the peninsular area [*Ardelan et al*., 2010]. In our study area, aeolian inputs of iron are also negligible because of the long distance from the continent or big islands. Moreover, during our study, sea-ice had already retreated to the south (as was evident from remote sensing data), and all stations were far away from the marginal ice zone. Therefore, we could expect that the main sources of iron supply to the upper water column were mixing and upwelling.

[31] From the results of iron enrichment incubations, *Hopkinson et al*. [2007] concluded that iron was not a limiting factor in shelf waters in the southern Drake Passage region. Mixing of a small amount of high-iron shelf waters with severely iron-depleted ACC waters is a plausible mechanism to maintain elevated phytoplankton biomass found downstream in the ACC. *Hopkinson et al*. [2007] hypothesized that phytoplankton blooms were the result of natural iron additions to ACC waters. *Dulaiova et al*. [2009] also reported that lateral iron supply were significantly higher than vertical upward fluxes in the southern Drake Passage. However, their study site was located south of the SACCF (northern region of Kr8; Figure 1), which was comparable to our stations Sf2 and Sf3. Iron deficiency may limit phytoplankton growth in pelagic Antarctic waters, but not in coastal waters close to the continent.

[32] Decadal scaled ocean color images show that higher chlorophyll-a concentrations occur mostly to the south of the PF and to the north of the SB, except for the Antarctic Peninsula shelf [*Park et al*., 2010]. Also, high chlorophyll-a concentrations around the South Shetland Islands extend as a band toward the northeast over the deep waters of the central portion of the Scotia Sea [*Ardelan et al*., 2010]. These data imply that natural iron fertilization may enhance primary production in the regions of topographic effects rather than in the vicinity of iron-rich waters.

[33] While surface F_v/F_m values did not covary with chlorophyll-a concentrations during our study, there was a spatial pattern of variability of F_v/F_m in relation to the topographic effects. For instance, the F_v/F_m values at the surface were high at Sf2 and Ws7, where nutrient concentrations were also higher than in the vicinity, though the surface chlorophyll-a concentrations were not (Table 2). The Sf2 station was located on the right side of Shackleton Transverse Ridge, which acts as a topographic barrier (against eastward flow of the ACC) capable of promoting vertical mixing [*Park et al*., 2010]. In case of Ws7, oceanic advection could bring a favorable nutritional condition through mixing. Shackleton Jet may stimulate mixing between the ACC and iron-replete shelf waters [*Zhou et al*., 2010]. In this context, the mixing processes may act as natural iron fertilization of downstream waters and be responsible for the elevated chlorophyll concentrations or quantum efficiencies of photosynthesis, F_v/F_m (e.g., at Ws7).

[34] Vertical transport of iron through upwelling or water mass intrusion may also bring new sources of iron to surface waters. *Peloquin and Smith* [2007] suggested that episodic intrusions of modified circumpolar deep waters from off the continental shelf into the euphotic zone in the southern Ross Sea could have supplied sufficient amount of iron to fuel diatom bloom in the summer. From their study in the Atlantic sector of the Southern Ocean, *Klunder et al*. [2011] also pointed out that vertical mixing and upwelling were the most important mechanisms of iron supply to the upper layer. However, *Hiscock et al*. [2003] noted that because the newly upwelled, iron-rich upper circumpolar deep water is only present at the surface north of the SB, the waters south of this front are iron poor. This may explain our observed low values of F_v/F_m (0.36) at Ws8, though chlorophyll-a concentration was elevated (0.90 mg m^{-3}).

[35] The maximum FRRF-derived values of F_v/F_m in nutrient-replete eukaryotic algae, including diatoms, are ~0.65 [*Kolber and Falkowski*, 1993]. The maximum values of F_v/F_m observed in iron-enriched waters of the SO are ~0.55 [*Coale et al*., 2004; *Gervais et al*., 2002]. In this study, the average F_v/F_m value was 0.38, thereby F_v/F_m varied from ~0.25 to ~0.43 in the ACC waters, and from ~0.32 to 0.42 in the shelf and the Southern Boundary of the ACC region, except for two stations with high F_v/F_m (~0.51). Our measured F_v/F_m values are, on average, lower than the previous observations in the SO. *Peloquin and Smith* [2007] reported F_v/F_m of 0.43 (average) in the Ross Sea, and they found exceptionally high F_v/F_m values

(0.5–0.65) for most of the seasonal phytoplankton bloom. *Fragoso and Smith* [2012] also observed relatively high value (mostly >0.4) in all blooms in the Ross Sea and the Amundsen Sea, with the maximum values >0.6. However, these observations were conducted in the austral summer and were obtained with a pulse amplitude modulation (PAM) fluorometer, which usually overestimates F_v/F_m readings by ~20%, compared with the FRRF. Although *Sedwick et al*. [2000] noted that iron concentrations in surface waters were relatively high at the beginning of the bloom mainly due to deep mixing and sea-ice melting, our results suggest that this may not be the case for the whole Scotia Sea. Our field measurements revealed physiological signatures of iron limitation in the western Scotia Sea even in the early austral summer.

4.3. F_v/F_m Related to Phytoplankton Communities

[36] Generally, larger size assemblages dominate nutrient-replete waters and phytoplankton blooms, such as the Antarctic PF and marginal ice zone [*Bracher et al*., 1999]. In contrast, nanophytoplankton and picophytoplankton tend to dominate open waters of the SO [*Froneman et al*., 2001; *Laubscher et al*., 1993; *Weber and El-Sayed*, 1987]. Iron enrichment stimulates a shift in the community structure toward larger diatoms (reviewed by *de Baar et al*. [2005]). *Suzuki et al*. [2002] also observed a dramatic floristic shift from phytoflagellates to diatoms during an iron enrichment experiment in the subarctic Pacific Ocean. The phytoplankton crop size on the shelf exhibits a seasonal change, with microplankton being dominant in December but nanoplankton dominant in February and March [*Holm-Hansen and Mitchell*, 1991]. However, in our study, diatoms were dominant only at Sf3, and *Phaeocystis* species prevailed (Figure 6). *Olson et al*. [2000] observed that, in the Ross Sea and the PF during late summer, cryptophytes almost always had high F_v/F_m and showed only minor responses to iron addition. In contrast, during our study, F_v/F_m was not high in the areas where *Cryptomonas* species predominated (Kr4 and Kr6), (Table 2). Although small cells, such as nanoflagellates and picoeukaryotes, better sequester trace elements such as iron [*Sunda and Huntsman*, 1997], there is an evidence that smaller cells may also be iron limited, although to a lesser extent [*Boyd and Abraham*, 2001; *Olson et al*., 2000]. *Phaeocystis antarctica* (a haptophyte with colonial and single-celled morphologies; predominant species in the Antarctic Sea) apparently has a greater demand for iron than diatoms [*Sedwick et al*., 2007]. Moreover, *P. antarctica* often dominates mixing zones because it has a better ability to maintain near-maximal photosynthetic rates at much lower irradiance levels than diatom do [*Arrigo et al*., 1999]. Therefore, our observations can be explained by the biochemical characteristics of *Phaeocystis*. During our study, *Phaeocystis* species were dominant at Sf2, Kr4, Ws7, and Ws8, where MLDs were deep (82, 70, 68, and 82 m, respectively; Table 2 and Figure 6).

[37] The majority of biological programs in the SO were conducted in the austral summer, from late December to February. In contrast, our study was conducted much earlier in the austral summer when iron limitation was expected to be less critical. However, our data suggest strong signatures of iron limitation of phytoplankton photophysiology at that season. On the contrary, the observed high values of F_v/F_m (>0.5) in near-surface phytoplankton at Sf2 and Ws7 stations suggest the importance of topographic effects related to hydrography. Although there are no reliable iron data, our results imply that not only light intensity but also iron availability is an important factor for phytoplankton growth phase in the study area.

[38] **Acknowledgments.** We thank the members of 15th Korean Antarctic Research Program onboard the R/V Yuzhmorgeologiya who collaborated on this research. This study was supported by KOPRI project PP13020. MYG was, in part, supported by the NASA Ocean Biology and Biogeochemistry Program. We also thank two anonymous reviewers and the Editor for their help in strengthening the manuscript.

References

Ardelan, M. V., O. Holm-Hansen, C. D. Hewes, C. S. Reiss, N. S. Silva, H. Dulaiova, E. Steinnes, and E. Sakshaug (2010), Natural iron enrichment around the Antarctic Peninsula in the Southern Ocean, *Biogeosciences*, *7*(1), 11–25.

Arrigo, K. R., and C. R. McClain (1994), Spring phytoplankton production in the western Ross Sea, *Science*, *266*(5183), 261–263.

Arrigo, K. R., and G. L. van Dijken (2003), Phytoplankton dynamics within 37 Antarctic coastal polynya systems, *J. Geophys. Res.*, *108*(C8), 3271, doi:10.1029/2002JC001739.

Arrigo, K. R., D. Worthen, A. Schnell, and M. P. Lizotte (1998), Primary production in Southern Ocean waters, *J. Geophys. Res.*, *103*(C8), 15,587–15,600.

Arrigo, K. R., D. H. Robinson, D. L. Worthen, R. B. Dunbar, G. R. DiTullio, M. VanWoert, and M. P. Lizotte (1999), Phytoplankton community structure and the drawdown of nutrients and CO2 in the Southern Ocean, *Science*, *283*, 365–367.

Barbini, R., F. Colao, R. Fantoni, L. Fiorani, A. Palucci, E. S. Artamonov, and M. Galli (2003), Remotely sensed primary production in the western Ross Sea: Results of in situ tuned models, *Antarct. Sci*, *15*(1), 77–84.

Bibby, T. S., M. Y. Gorbunov, K. W. Wyman, and P. G. Falkowski (2008), Photosynthetic community responses to upwelling in mesoscale eddies in the subtropical North Atlantic and Pacific Oceans, *Deep Sea Res. Part II*, *55*(10-13), 1310–1320.

Blain, S., et al. (2007), Effect of natural iron fertilization on carbon sequestration in the Southern Ocean, *Nature*, *446*(7139), 1070–1074.

Boyd, P. W. (2002), The role of iron in the biogeochemistry of the Southern Ocean and equatorial Pacific: A comparison of in situ iron enrichments, *Deep Sea Res. Part II*, *49*(9-10), 1803–1821.

Boyd, P. W., and E. R. Abraham (2001), Iron-mediated changes in phytoplankton photosynthetic competence during SOIREE, *Deep Sea Res. Part II*, *48*(11-12), 2529–2550.

Bracher, A. U., B. M. A. Kroon, and M. I. Lucas (1999), Primary production, physiological state and composition of phytoplankton in the Atlantic Sector of the Southern Ocean, *Mar. Ecol. Prog. Ser.*, *190*, 1–16.

Breugem, W. P., P. Chang, C. J. Jang, J. Mignot, and W. Hazeleger (2008), Barrier layers and tropical Atlantic SST biases in coupled GCMs, *Tellus A*, *60*(5), 885–897.

Coale, K. H., et al. (2004), Southern Ocean iron enrichment experiment: Carbon cycling in high- and low-Si waters, *Science*, *304*(5669), 408–414.

Crumpton, W. G. (1987), A simple and reliable method for making permanent mounts of phytoplankton for light and fluorescence microscopy, *Limnol. Oceanogr.*, *32*(5), 1154–1159.

de Baar, H. J. W., J. T. M. de Jong, D. C. E. Bakker, B. M. Loscher, C. Veth, U. Bathmann, and V. Smetacek (1995), Importance of iron for plankton blooms and carbon dioxide drawdown in the Southern Ocean, *Nature*, *373*(6513), 412–415.

de Baar, H. J. W., et al. (2005), Synthesis of iron fertilization experiments: From the Iron Age in the Age of Enlightenment, *J. Geophys. Res.*, *110*, C09S16, doi:10.1029/2004JC002601.

Dulaiova, H., M. V. Ardelan, P. B. Henderson, and M. A. Charette (2009), Shelf-derived iron inputs drive biological productivity in the southern Drake Passage, *Global Biogeochem. Cycles*, *23*, GB4014, doi:10.1029/2008GB003406.

El-Sayed, S. Z. (2005), History and evolution of primary productivity studies of the Southern Ocean, *Polar Biol.*, *28*(6), 423–438.

Falkowski, P. G., M. Koblizek, M. Gorbunov, and Z. Kolber (2004), ›Development and Application of Variable Chlorophyll Fluorescence Techniques in Marine Ecosystems, in *Chlorophyll a Fluorescence: A signature of Photosynthesis*, edited by C. Papageorgiou and Govingjee, pp. 757–778, Springer, Dordrecht.

Falkowski, P. G., and Z. Kolber (1995), Variations in chlorophyll fluorescence yields in phytoplankton in the world oceans, *Aust. J. Plant Physiol.*, *22*(2), 341–355.

Fragoso, G. M., and W. O. Smith Jr (2012), Influence of hydrography on phytoplankton distribution in the Amundsen and Ross Seas, Antarctica, *J. Mar. Syst.*, *89*(1), 19–29.

Froneman, P. W., R. K. Laubscher, and C. D. McQuaid (2001), Size-fractionated primary production in the south Atlantic and Atlantic sectors of the Southern Ocean, *J. Plankton Res.*, *23*(6), 611–622.

Fuchs, E., R. C. Zimmerman, and J. S. Jaffe (2002), The effect of elevated levels of phaeophytin in natural water on variable fluorescence measured from phytoplankton, *J. Plankton Res.*, *24*(11), 1221–1229.

Garcia, H. E., R. A. Locarnini, T. P. Boyer, and J. I. Antonov (2006), World Ocean Atlas 2005, vol. *4*: *Nutrients (Phosphate, Nitrate, and Silicate)*, 396 pp, NODC-NOAA (National Oceanographic Data Center - National Oceanic and Atmospheric Administration), Washington, D. C.

Gervais, F., U. Riebesell, and M. Y. Gorbunov (2002), Changes in primary productivity and chlorophyll a in response to iron fertilization in the Southern Polar Frontal Zone, *Limnol. Oceanogr.*, *47*(5), 1324–1335.

Greene, R. M., R. J. Geider, Z. Kolber, and P. G. Falkowski (1992), Iron-induced changes in light harvesting and photochemical energy conversion processes in eukaryotic marine algae, *Plant Physiol.*, *100*(2), 565–575.

Hiscock, M. R., J. Marra, W. O. Smith, R. Goericke, C. Measures, S. Vink, R. J. Olson, H. M. Sosik, and R. T. Barber (2003), Primary productivity and its regulation in the Pacific Sector of the Southern Ocean, *Deep Sea Res. Part II*, *50*(3-4), 533–558.

Hiscock, M. R., V. P. Lance, A. M. Apprill, R. R. Bidigare, Z. I. Johnson, B. G. Mitchell, W. O. Smith, and R. T. Barber (2008), Photosynthetic maximum quantum yield increases are an essential component of the Southern Ocean phytoplankton response to iron, *Proc. Natl. Acad. Sci. U. S. A.*, *105*(12), 4775–4780.

Holm-Hansen, O., and B. G. Mitchell (1991), Spatial and temporal distribution of phytoplankton and primary production in the western Bransfield Strait region, *Deep Sea Res. Part I*, *38*(8-9), 961–980.

Holm-Hansen, O., et al. (2004), Factors influencing the distribution, biomass, and productivity of phytoplankton in the Scotia Sea and adjoining waters, *Deep Sea Res. Part II*, *51*(12-13), 1333–1350.

Hopkinson, B. M., G. Mitchell, R. A. Reynolds, H. Wang, K. E. Selph, C. I. Measures, C. D. Hewes, O. Holm-Hansen, and K. A. Barbeau (2007), Iron limitation across chlorophyll gradients in the southern Drake Passage: Phytoplankton responses to iron addition and photosynthetic indicators of iron stress, *Limnol. Oceanogr.*, *52*(6), 2540–2554.

Hoppema, M., H. J. W. de Baar, E. Fahrbach, H. H. Hellmer, and B. Klein (2003), Substantial advective iron loss diminishes phytoplankton production in the Antarctic Zone, *Global Biogeochem. Cycles*, *17*(1), 1025, doi:10.1029/2002GB001957.

Kang, S. H., J. S. Kang, S. Lee, K. H. Chung, D. Kim, and M. G. Park (2001), Antarctic phytoplankton assemblages in the marginal ice zone of the northwestern Weddell Sea, *J. Plankton Res.*, *23*(4), 333–352.

Klunder, M. B., P. Laan, R. Middag, H. J. W. De Baar, and J. C. van Ooijen (2011), Dissolved iron in the Southern Ocean (Atlantic sector), *Deep Sea Res. Part II*, *58*(25-26), 2678–2694.

Kolber, Z., and P. G. Falkowski (1993), Use of active fluorescence to estimate phytoplankton photosynthesis in situ, *Limnol. Oceanogr.*, *38*(8), 1646–1665.

Kolber, Z., J. Zehr, and P. Falkowski (1988), Effects of growth irradiance and nitrogen limitation on photosynthetic energy conversion in photosystem II, *Plant Physiol.*, *88*(3), 923–929.

Laubscher, R. K., R. Perissinotto, and C. D. Mcquaid (1993), Phytoplankton production and biomass at frontal zones in the Atlantic sector of the Southern Ocean, *Polar Biol.*, *13*(7), 471–481.

Marrari, M., C. Hu, and K. Daly (2006), Validation of SeaWiFS chlorophyll a concentrations in the Southern Ocean: A revisit, *Remote Sens. Environ.*, *105*(4), 367–375.

Martin, J. H., and S. E. Fitzwater (1988), Iron deficiency limits phytoplankton growth in the north-east Pacific subarctic, *Nature*, *331*(6154), 341–343.

Martin, J. H., R. M. Gordon, and S. E. Fitzwater (1990), Iron in Antarctic waters, *Nature*, *345*(6271), 156–158.

Menden-Deuer, S., and E. J. Lessard (2000), Carbon to volume relationships for dinoflagellates, diatoms, and other protist plankton, *Limnol. Oceanogr.*, *45*(3), 569–579.

Meredith, M. P., J. L. Watkins, E. J. Murphy, P. Ward, D. G. Bone, S. E. Thorpe, S. A. Grant, and R. S. Ladkin (2003), Southern ACC Front to the northeast of South Georgia: Pathways, characteristics, and fluxes, *J. Geophys. Res.*, *108*(C5), 3162, doi:10.1029/2001JC001227.

Mitchell, B. G., and O. Holm-Hansen (1991), Observations of modeling of the Antartic phytoplankton crop in relation to mixing depth, *Deep Sea Res. Part A*, *38*(8-9), 981–1007.

Mongin, M., E. Molina, and T. W. Trull (2008), Seasonality and scale of the Kerguelen plateau phytoplankton bloom: A remote sensing and modeling analysis of the influence of natural iron fertilization in the Southern Ocean, *Deep Sea Res. Part II*, *55*(5-7), 880–892.

Moore, J. K., and M. R. Abbott (2000), Phytoplankton chlorophyll distributions and primary production in the Southern Ocean, *J. Geophys. Res.*, *105*(C12), 28,709–28,722.

Moore, J. K., M. R. Abbott, and J. G. Richman (1997), Variability in the location of the Antarctic Polar Front (90°–20°W) from satellite sea surface temperature data, *J. Geophys. Res.*, *102*(C13), 27,825–27,833.

Moore, J. K., M. R. Abbott, and J. G. Richman (1999), Location and dynamics of the Antarctic Polar Front from satellite sea surface temperature data, *J. Geophys. Res.*, *104*(C2), 3059–3073.

Olaizola, M., R. J. Geider, W. G. Harrison, L. M. Graziano, G. M. Ferrari, and P. M. Schlittenhardt (1996), Synoptic study of variations in the fluorescence-based maximum quantum efficiency of photosynthesis across the North Atlantic Ocean, *Limnol. Oceanogr.*, *41*(4), 755–765.

Olson, R. J., H. M. Sosik, A. M. Chekalyuk, and A. Shalapyonok (2000), Effects of iron enrichment on phytoplankton in the Southern Ocean during late summer: Active fluorescence and flow cytometric analyses, *Deep Sea Res. Part II*, *47*(15-16), 3181–3200.

Orsi, A. H., T. Whitworth, and W. D. Nowlin (1995), On the meridional extent and fronts of the Antarctic Circumpolar Current, *Deep Sea Res.*, *42*(5), 641–673.

Park, J., I.-S. Oh, H.-C. Kim, and S. Yoo (2010), Variability of SeaWiFs chlorophyll-a in the southwest Atlantic sector of the Southern Ocean: Strong topographic effects and weak seasonality, *Deep Sea Res.*, *57*(4), 604–620.

Parsons, T. R., Y. Maita, and C. M. Lalli (1984), *A Manual of Chemical and Biological Methods for Seawater Analysis*, Pergamon, Oxford and New York.

Peloquin, J. A., and W. O. Smith Jr. (2007), Phytoplankton blooms in the Ross Sea, Antarctica: Interannual variability in magnitude, temporal patterns, and composition, *J. Geophys. Res.*, *112*, C08013, doi:10.1029/2006JC003816.

Petrou, K., C. S. Hassler, M. A. Doblin, K. Shelly, V. Schoemann, R. van den Enden, S. Wright, and P. J. Ralph (2011), Iron-limitation and high light stress on phytoplankton populations from the Australian Sub-Antarctic Zone (SAZ), *Deep Sea Res. Part II*, *58*(21-22), 2200–2211.

Price, J. F., R. A. Weller, and R. Pinkel (1986), Diurnal cycling: Observations and models of the upper ocean response to diurnal heating, cooling, and wind mixing, *J. Geophys. Res.*, *91*(C7), 8411–8427.

Raven, J. A., M. C. W. Evans, and R. E. Korb (1999), The role of trace metals in photosynthetic electron transport in O2-evolving organisms, *Photosynthesis Res.*, *60*(2), 111–150.

Sedwick, P. N., G. R. DiTullio, and D. J. Mackey (2000), Iron and manganese in the Ross Sea, Antarctica: Seasonal iron limitation in Antarctic shelf waters, *J. Geophys. Res.*, *105*(C5), 11,321–11,336.

Sedwick, P. N., N. Garcia, S. Riseman, C. Marsay, and G. R. DiTullio (2007), Evidence for high iron requirements of colonial Phaeocystis antarctica at low irradiance, *Biogeochemistry*, *83*(1), 83–97.

Smith, K. L., B. H. Robison, J. J. Helly, R. S. Kaufmann, H. A. Ruhl, T. J. Shaw, B. S. Twining, and M. Vernet (2007), Free-drifting icebergs: Hot spots of chemical and biological enrichment in the Weddell Sea, *Science*, *317*(5837), 478–482.

Smith, W. O., Jr., and L. I. Gordon (1997), Hyperproductivity of the Ross Sea (Antarctica) polynya during austral spring, *Geophys. Res. Lett.*, *24*(3), 233–236.

Smith, W. O., J. Marra, M. R. Hiscock, and R. T. Barber (2000), The seasonal cycle of phytoplankton biomass and primary productivity in the Ross Sea, Antarctica, *Deep Sea Res. Part II*, *47*(15-16), 3119–3140.

Sosik, H. M., and R. J. Olson (2002), Phytoplankton and iron limitation of photosynthetic efficiency in the Southern Ocean during late summer, *Deep Sea Res.*, *49*(7), 1195–1216.

Sprintall, J. (2003), Seasonal to interannual upper-ocean variability in the Drake Passage, *J. Mar. Res.*, *61*(1), 27–57.

Sullivan, C. W., K. R. Arrigo, C. R. McClain, J. C. Comiso, and J. Firestone (1993), Distributions of phytoplankton blooms in the Southern Ocean, *Science*, *262*(5141), 1832–1837.

Sunda, W. G., and S. A. Huntsman (1997), Interrelated influence of iron, light and cell size on marine phytoplankton growth, *Nature*, *390*(6658), 389–392.

Suzuki, K., H. Liu, T. Saino, H. Obata, M. Takano, K. Okamura, Y. Sohrin, and Y. Fujishima (2002), East-west gradients in the

photosynthetic potential of phytoplankton and iron concentration in the Subarctic Pacific Ocean during early summer, *Limnol. Oceanogr.*, *47*(6), 1581–1594.

Vassiliev, I. R., Z. Kolber, K. D. Wyman, D. Mauzerall, V. K. Shukla, and P. G. Falkowski (1995), Effects of iron limitation on photosystem II composition and light utilization in Dunaliella tertiolecta, *Plant Physiol.*, *109*(3), 963–972.

Weber, L. H., and S. Z. El-Sayed (1987), Contributions of the net, nano- and picoplankton to the phytoplankton standing crop and primary productivity in the Southern Ocean, *J. Plankton Res.*, *9*(5), 973–994.

Westwood, K. J., F. Brian Griffiths, K. M. Meiners, and G. D. Williams (2010), Primary productivity off the Antarctic coast from 30°-80°E; BROKE-West survey, 2006, *Deep Sea Res. Part II*, *57*(9-10), 794–814.

Wulff, A., and S. Å. Wängberg (2004), Spatial and vertical distribution of phytoplankton pigments in the eastern Atlantic sector of the Southern Ocean, *Deep Sea Res. Part II*, *51*(22-24), 2701–2713.

Zhou, M., Y. Zhu, R. D. Dorland, and C. I. Measures (2010), Dynamics of the current system in the southern Drake Passage, *Deep Sea Res.*, *57*(9), 1039–1048.